ISSN: 1692-7257 - Volume 2 – Issue 48 - 2026

ORIGINAL

RCTA
Revista Colombiana de Tecnologías de Avanzada
UNIPAMPLONA

Multi-species mathematical modeling and dynamic simulation of a microbial electrolysis cell for biohydrogen production

Modelado matemático multiespecie y simulación dinámica de una celda de electrólisis microbiana para la producción de biohidrógeno

Juan Carlos Quintero Díaz[1]
Diego Fernando Mendoza Muñoz[1]

[1] **Universidad de Antioquia, Departamento de Ingeniería Química, Medellín, Antioquia, Colombia.**

Received: 27 March 2026. Revised: 12 May 2026. Accepted: 12 June 2026. Published: 02 July 2026.
Corresponding Author: Juan Carlos Quintero Díaz

How to cite: J. C. Quintero Díaz and D. F. Mendoza Muñoz, "Modelado matemático multiespecie y simulación dinámica de una celda de electrólisis microbiana para la producción de biohidrógeno", *Revista Colombiana de Tecnologías de Avanzada (RCTA)*, vol. 2, no. 48, jul. 2026, art. no. 4391, doi: 10.24054/rcta.v2i48.4391

This work is licensed under a Creative Commons Attribution-NonCommercial 4.0 International License.

Abstract:

A multi-population mathematical model was developed to analyze hydrogen production in Microbial Electrolysis Cells (MECs) under continuous operation. The model, implemented in Python, integrates the dynamics of fermentative, methanogenic, and exoelectrogenic bacteria with the electrochemical phenomena of the cell, and enabled assessment of the effects of applied voltage and substrate concentration on system performance. The results from the model show that exoelectrogenic bacteria form a mature biofilm that reduces the internal resistance of the cell, achieving hydrogen flow rates of 400 mL/d at 1.0 V and a Coulombic efficiency of 60%. The findings derived from the model represent a relevant contribution toward the optimization and industrial scale-up of this technology.

Keywords: hydrogen, microbial electrolysis cells, methane, Coulombic efficiency, mathematical modelling.

Resumen:

Se desarrolló un modelo matemático multipoblacional para analizar la producción de hidrógeno en Celdas de Electrólisis Microbiana (CEM) en operación continua. El modelo, implementado en Python, integra la dinámica de bacterias fermentativas, metanogénicas y electrogénicas con los fenómenos electroquímicos de la celda, y permitió evaluar el efecto del voltaje aplicado y la concentración de sustrato sobre el desempeño del sistema. Los resultados del modelo muestran que las bacterias electrogénicas forman una biopelícula madura que reduce la resistencia interna de la celda, alcanzando flujos de hidrógeno de 400 mL/d a 1,0 V y una eficiencia coulómbica del 60%. Los hallazgos derivados del modelo constituyen una contribución relevante para la optimización y el escalamiento industrial de esta tecnología.

Palabras clave: hidrógeno, celdas de electrólisis microbianas, metano, eficiencia Coulómbica, modelado matemático.

INTRODUCTION

The intensive use of fossil fuels represents the main cause of environmental deterioration, generating various problems for human health and effects on ecosystems [1], [2]. Currently, the global energy matrix continues to depend for more than 80% on non-renewable sources such as oil, coal and natural gas [3]. In this scenario, hydrogen (H_2) emerges as a strategic energy vector, and it is projected that by the year 2050 it could supply 10% of the energy consumed globally [4]. However, the current challenge lies in its method of production: 96% of global hydrogen production comes from thermochemical processes that use fossil fuels, such as methane reforming [5]. An innovative alternative is the technology of Microbial Electrolysis Cells (CEM or MEC, by its English acronym). These cells allow hydrogen to be produced with significantly lower energy consumption than conventional electrolysis [6].

The operating principle of a Microbial Electrolysis Cell (CEM) is based on the metabolic activity of exoelectrogenic bacteria. These microorganisms oxidize organic matter and transfer the resulting electrons to the anode of an electrochemical circuit. Subsequently, through the application of an external voltage (typically between 0.3 and 1.0 V), the electrons migrate to the cathode, where the protons (H^+) present in the medium are reduced to produce hydrogen gas (H_2)[7],[8].

The viability of MEC cells is enhanced when wastewater from various sources — urban, agricultural, dairy and industrial — is used as a low-cost substrate for hydrogen production. Wastewater has been found to contain between 3 and 10 times the energy required for its own treatment, stored mainly as organic matter (approx. 1.79 kWh/m³), nutrients and thermal energy [9], [10], [11].

In a CEM, the reported hydrogen production values range between 0.01-3.9 m^3 H_2/m^3 d, using acetate and with an applied voltage of 1.0 V [12], [13]. Despite its potential, the use of wastewater in a CEM requires the analysis of the variables that affect its efficiency and scaling up [14].

In this context, mathematical modelling is presented as a tool for understanding the dynamic relationship between the biodegradation of organic matter, the growth of microbial populations and the electrochemical phenomena occurring in a CEM. The mathematical description of these processes is essential for the design, optimization and industrial scaling up of the technology[15],[16].

The CEM models that have been proposed are based on electrochemical and biological principles, which have previously been applied to microbial fuel cells. Historically, most efforts have been devoted to the modelling of microbial fuel cells[17],[18],[19], but models have also been developed for microbial electrolysis cells[16], microbial electrosynthesis cells [20] and desalination cells[21].

These models are based on ordinary differential equations of species balance, with Monod-type kinetics and the use of Faraday's law and the Nernst equation as electrochemical models. The models have evolved to include not only analyses of temporal dynamics, 0D, but also 1D, 2D and 3D analyses that employ partial differential equations to study the spatial distribution of substrates and biomass[22],[23]. In addition, the operation of these bioelectrochemical cells in batch, fed-batch and continuous operation has been modeled[16],[24],[25]. Single-chamber cells without the use of a membrane[19], [26] and two-chamber cells[27],[28]have also been modeled.

The models have also incorporated the presence of pure cultures simulating the behavior of strains such as Shewanella or G. sulfurreducens[18],[22], [27], or models with multi-species systems simulating the presence of bacterial consortia as in the case of anaerobic sludge[16], [23]. Electron transfer strategies have also been included, comprising direct transfer mechanisms[22] as well as the use of intracellular [16] or extracellular[18]mediators. The model of Pinto et al. [16] was the first dynamic multi-population model capable of simulating hydrogen production (H_2) from complex organic matter in a single-chamber MEC operated continuously. The model uses ordinary differential equations to describe the growth and metabolic activity of four microbial populations interacting as a biofilm around the electrodes. Table 1 summarizes the most important factors that have been considered in the modeling of microbial cells.

The highly nonlinear nature derived from the complexity of the dynamics observed in bioelectrochemical cells represents a challenge for parametric identification and system control. In response to these limitations, hybrid approaches that integrate mechanistic models with machine learning techniques, such as recurrent neural networks, have emerged as alternatives to improve predictive accuracy and real-time control [29], [30], [31], although their "black box" nature limits physical interpretability. Consequently, the development of more refined models that integrate the description of the biofilm, the dynamic behavior of mass and charge, and the efficiency of the reactor continues to be a priority need in order to advance toward the scaling and rational optimization of microbial electrolysis cells.

This work proposes a mathematical model that integrates the three phenomena described above for a dual-chamber CEM under continuous operation, with the aim of identifying its dynamic behavior and evaluating the effect of variables such as the applied voltage and the organic matter feed on hydrogen production and the Coulombic efficiency of the system.

Table 1: Factors considered in the mathematical models of microbial electrolysis cells

Criterion	Options			This work
Dimension	0D	1D / 2D / 3D		0D
Chambers	Anode	Cathode	Anode/Cathode	Anode/Cathode
EET	Direct	Endogenous mediator	Exogenous mediator	Endogenous mediator
Culture	Pure	Two species	Consortium	Consortium
Operation	Batch	Fed batch	Continuous	Continuous

METHODOLOGY

Description of the MEC

The model proposed in this work is an adaptation of the model of Pinto et al. [16], with the aim of describing a dual-chamber CEM (Figure 1), where, unlike the model of Pinto et al., the cathode does not contain a microbial biofilm and therefore there is no H2 consumption or CH4 formation. Additionally, the flocculent biomass is considered to be in suspension and as a biofilm on the anode, such that the fraction of the biomass leaving in the effluent is represented by the parameter α (equations 3 to 5). Wastewater containing organic matter represented by glucose (S) and acetate (A) enters the anodic chamber and leaves as effluent with a significant reduction in organic matter.

The anaerobic sludge is either attached to the electrode, forming a biofilm, or suspended in the medium, and consists of three types of bacterial species: fermentative (x_f), methanogenic (x_m) and exoelectrogenic (x_e), in that order from highest to lowest proportion in the sludge biomass. These species carry out the following conversion reactions:

Conversion of glucose into acetate by fermentative bacteria (x_f):

$C_6H_{12}O_6$ (S)→ $3C_2H_4O_2$ (A)

Acetate consumption by methanogenic bacteria (x_m):

$C_2H_4O_2$ (A) → $CH_4 + CO_2$

Acetate consumption by exoelectrogenic bacteria (x_e):

$C_2H_4O_2$ (A) + $2H_2O$ + 4Mox → 4Mred + $2CO_2$

In this last reaction, exoelectrogenic bacteria are considered to endogenously produce a redox mediator (M) that facilitates electron transfer from the interior of the cell to the anode [32], [33], [34].

The electrons delivered by the exoelectrogenic bacteria to the anode are driven by an external energy source toward the cathode, while the protons released during the oxidation of organic matter also flow toward the cathode through a semipermeable membrane that separates the two chambers. The hydrogen formation reaction at the cathode is as follows:

$2H^+ + 2e^- \rightarrow H_2(g)$

The theoretical thermodynamic potential of an MEC (E_{CEF}) for hydrogen production at pH 7.0 is -0.14 V, so the reaction is not spontaneous and an external potential greater than 0.14 V must be applied for hydrogen production to take place; however, the overpotentials of the cell require the application of a voltage higher than 0.2 to 1.0 V [6].

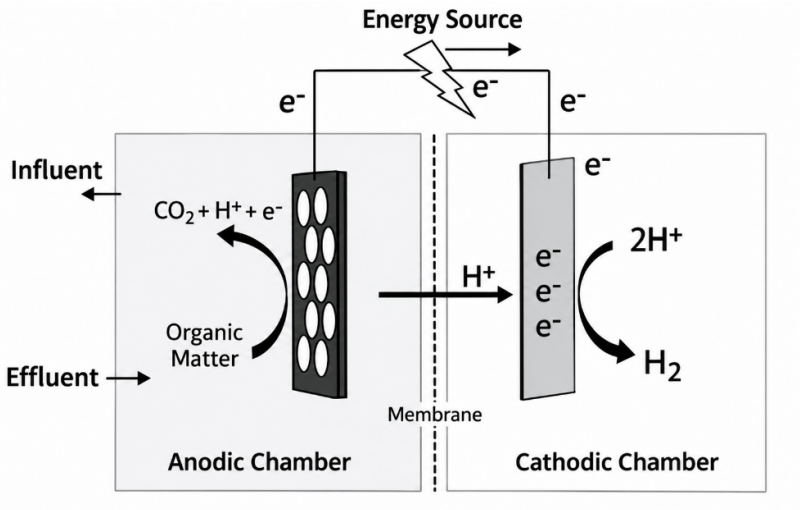

Fig. 1. *Schematic of a dual-chamber MEC for hydrogen production.*

The mass balances for a continuous-flow MEC (Figure 1) are described in equations 1-7. For the cell balance, it is considered that these do not leave the reactor because they are either attached to the electrode or settle in the medium.

Substrate balance (S) $\frac{dS}{dt} = -q_f x_f + D(S_0 - S)$ Eq. 1

Acetate balance (A): $\frac{dA}{dt} = -q_e x_e - q_m x_m + Y_{COD} q_f x_f + D(A_0 - A)$ Eq. 2

Balance of fermentative bacteria (x_f) $\frac{dx_f}{dt} = \mu_f x_f - K_{df} x_f - \alpha x_f$ Eq. 3

Balance of acetoclastic methanogenic bacteria (x_m) $\frac{dx_m}{dt} = \mu_m x_m - K_{dm} x_m - \alpha x_m$ Eq. 4

Exoelectrogenic bacteria balance (x_e) $\frac{dx_e}{dt} = \mu_e x_e - K_{de} x_e - \alpha x_e$ Eq. 5

Endogenous redox mediator balance (M) $M_{Total} = M_{red} + M_{ox}$ Eq. 6

$\frac{dM_{ox}}{dt} = -Y_M q_e + \frac{\gamma}{V x_e} \frac{I_{MEC}}{nF}$ Eq. 7

The growth (μ_i) and substrate consumption (q_i) kinetics based on the Monod model correspond to equations 8-13.

$\mu_f = \mu_{máx,f} \frac{S}{K_{s,f} + S}$ Eq. 8

$\mu_e = \mu_{máx,e} \frac{A}{K_{A,e} + A}$ Eq. 9

$\mu_m = \mu_{máx,m} \frac{A}{K_{A,m} + A}$ Eq. 10

$q_f = q_{máx,f} \frac{S}{K_{s,f} + S}$ Eq. 11

$q_e = q_{máx,e} \frac{A}{K_{A,e} + A}$ Eq. 12

The electrochemical balance of the cell is described in equations 14 to 19, where the applied voltage $E_{app.}$ must be sufficient to cover the thermodynamic potential E_{CEF}. The ohmic overpotential (η_{ohm}), based on Ohm's law, represents the energy lost as heat due to the difficulty of ions moving through the liquid (electrolyte) and the membrane, and of electrons through the wires and electrodes. The anodic overpotential (η_a), based on the Nernst equation applied to the biological mediator, represents the potential loss that occurs due to the limited rate of mediator reduction, while the cathodic overpotential (η_c) is a form of the Butler-Volmer equation that represents the energy required to maintain the chemical reaction on the cathode surface. R_{int} is represented by an empirical model proposed by Marcus and colleagues in 2007 [35], which proposes that the internal resistance decreases as the biomass of exoelectrogenic bacteria at the anode increases.

The rate of methane production (Q_{CH4}) in the anode and hydrogen chamber (Q_{H2}) in the cathodic chamber they are represented by equations 20 and 21.

$-E_{aplic.} = E_{CEF} - \eta_{ohm} - \eta_a - \eta_c$ Eq. 14

$\eta_{ohm} = I_{MEC} * R_{int}$ Eq. 15

$\eta_a = \frac{RT}{nF} \ln\left(\frac{M_{total}}{M_{red}}\right)$ Eq. 16

$\eta_c = \frac{RT}{\beta_m F} \sinh^{-1}\left(\frac{I_{MEC}}{A_e\, i_0}\right)$ Eq. 17

$I_{MEC} = \frac{E_{CEF} + E_{app.} - \eta_a - \eta_c}{R_{int}}$ Eq. 18

$R_{int} = R_{\min} + (R_{\max} - R_{\min})\, e^{-K_R x_e}$ Eq. 19

$Q_{CH4} = Y_{CH4}\, q_m\, x_m\, V$ Eq. 20

$Q_{H2} = Y_{H2} \left(\frac{I_{MEC}}{nF} \frac{RT}{P}\right)$ Eq. 21

The kinetic and electrochemical parameters were adapted from the values validated by Pinto et al. [16] and are presented in Table 2.

Numerical solution of the model

The system of ordinary differential equations was solved by numerical computation in the Python environment, using the variable-step integration algorithm odeint from the SciPy library. To evaluate the impact of the parameters on hydrogen production, a local sensitivity analysis was performed by perturbing each model parameter by 1% while keeping the others constant. The dynamic results were normalized and averaged over time using the RMS (Root Mean Square) metric. Finally, the parameters were ranked in a Pareto diagram to clearly identify the critical variables of the system [36], [37]. The initial conditions of the dynamic variables used were: So = 1000 mg/L; Ao = 10 mg/L; x_{fo}=50 mg/L; x_{mo}= 20 mg/L; x_{eo}= 5 mg/L; M_{ox}= 0.02 mg/L. The model was solved at a dilution rate (D) of 0.5 1/d, with a volume (V_{liq}) of 1 L in each chamber of the cell. The model was used to evaluate the effect of voltage and substrate concentration on H_2 production, the H_2 yield on substrate ($Y_{\frac{H_2}{S}}$) and the Coulombic efficiency (EC). These variables are defined in equations 22 and 23. To determine which parameters exert the greatest influence on the output variables (Q_{H2}, and EC), a global sensitivity analysis based on the RMS of the normalized sensitivities was performed [36], [37].

Table 2: Parameters used in the model

Parameter	Description	Value
$\mu_{max,f}$(1/d)	Maximum growth rate	0.15
$\mu_{max,e}$(1/d)	Maximum growth rate	0.25
$\mu_{max,m}$(1/d)	Maximum growth rate	0.1
$K_{s,f}$(mg/L)	Mean affinity constant	100
$K_{s,e}$(mg/L)	Mean affinity constant	20
$K_{s,m}$(mg/L)	Mean affinity constant	80
$q_{max,f}$(1/d)	Max. substrate consumption rate	16.0
$q_{max,e}$(1/d)	Max. substrate consumption rate	14.0
$q_{max,m}$(1/d)	Max. substrate consumption rate	14.0
$K_{d,f}$(1/d)	Decay rate	0.01
$K_{d,e}$(1/d)	Decay rate	0.01
$K_{d,m}$(1/d)	Decay rate	0.01
α (1/d)	Biomass washout rate	0.1
Y_{COD}(mg/mg)	Acetate/glucose yield	0.75
Y_M(mg/mg)	Ox. mediator yield	36.6
Y_{H2}(-)	Cathodic efficiency	0.8
Y_{CH4}(L/mg)	Methane yield	0.28
γ (-)	Transfer efficiency electrons	1.0
E_{CEL}(V)	Electromotive force \u200b	-0.3
Eapp (V)	Applied voltage to the cell	0.8
R_{min}(Ohm)	Minimum internal resistance	20
R_{max}(Ohm)	Maximum internal resistance	2000
K (L/mg)	Biomass resistance decay	0.024
F (C/mol e)	Faraday constant	96485
n (mol e/mol)	Electrons transferred	2
R (J/mol K)	Ideal gas constant	8.314
T (K)	Temperature	303.15
P (Pa)	Pressure	101325
M_{total}(M)	Total mediator conc.	0.05
V_{liq}(L)	Liquid volume	1.0
D (1/d)	Dilution rate	0.5
S_0(mg/L)	Influencing substrate concentration	3000
A_0(mg/L)	Influent acetate conc.	10
β_m(-)	Cathode charge transfer	0.5
A_c(m^2)	Cathode surface area	0.22
i_0(A/m^2)	Exchange current density	1.0

Source: The parameter values were taken in accordance with the orders of magnitude presented in [16].

$$Y_{\frac{H_2}{s}} = \frac{Q_{H2}}{D(So - S)} \quad \text{Eq. 22}$$

$$EC = \frac{I_{MEC}}{n\,F q_e x_e V} \quad \text{Eq. 23}$$

RESULTS AND DISCUSSION

Figures 2-5 present the dynamic behavior of a microbial electrolysis cell (CEM) in which the anode chamber is continuously fed with wastewater containing an organic load represented by glucose and acetate.

The dynamics of the microbial populations in the anode chamber show a clear transition from a heterogeneous inoculum toward a specialized community (Figure 2).

At the start of operation, the largest proportion of species corresponds to fermentative ones, which dominate the hydrolysis and acidogenesis stage, transforming the complex substrate (glucose) into metabolic intermediates such as acetate (Figure 3). This initial hierarchy, in which fermenters predominate over methanogenic organisms and these in turn over exoelectrogenic ones, is characteristic of conventional anaerobic sludge used as inoculum[38].

As the process progresses, a sigmoidal increase in the biomass of exoelectrogenic bacteria is observed (Figure 2). This growth is due to the thermodynamic advantage offered by the applied potential $E_{app.}$, which induces the anode to accept electrons. This allows exoelectrogenic bacteria to achieve a growth rate higher than that of their competitors under the established operating conditions.

On the other hand, the glucose turnover rate allows an active fermentative population to be maintained that consumes glucose and keeps its concentration low by transforming it into acetate. Due to glucose consumption, acetate initially tends to accumulate in the medium (Figure 3) owing to the low consumption by methanogenic and exoelectrogenic organisms, which are present in a low proportion in the medium; under these conditions, however, methanogenic organisms consume acetate, generating methane in significant proportions (Figure 4). However, as the growth of exoelectrogenic organisms increases, competition for acetate becomes greater, leading to a reduction in methane production and an increase in hydrogen production (Figure 4) due to electron transfer from the anode.

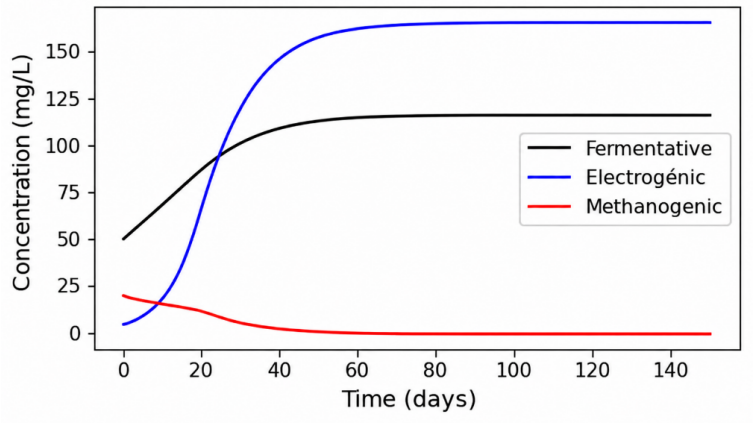

Fig. 2. *Behavior of bacterial species in the anode chamber of an MEC*

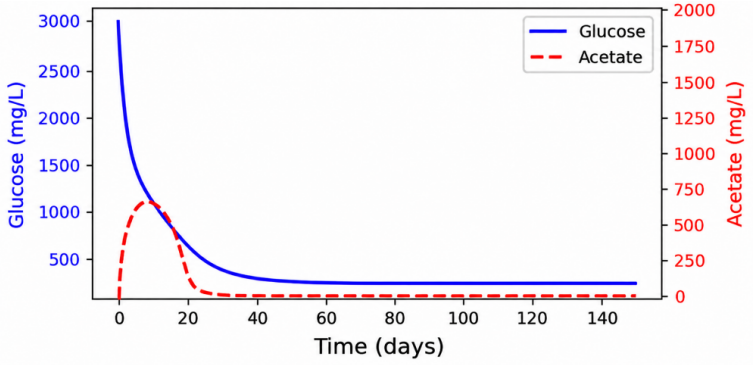

Fig. 3. *Glucose and acetate profiles in the anode chamber of an MEC*

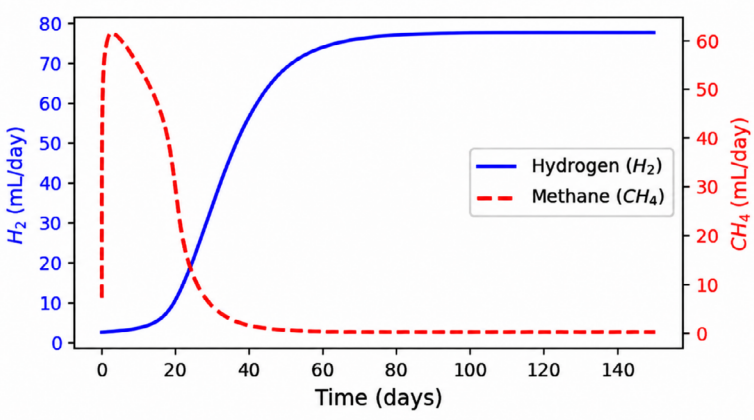

Fig. 4. *Dynamics of methane (anode chamber) and hydrogen (cathode chamber) evolution in an MEC*

Figure 5 presents the behavior of the current flow through the CEM and the internal resistance of the system. As the exoelectrogenic bacteria population grows and forms a mature biofilm (around day 20 to 40), a drastic drop in resistance is observed, which stabilizes at a minimum value close to 100 Ω. This reduction in resistance allows the current to increase in parallel. This phenomenon occurs because the biofilm acts as a biological catalyst that facilitates extracellular electron transfer, reducing the resistance to electron transfer to the anode. The adaptation of anaerobic sludge into an exoelectrogenic population has been reported in different studies[39],[40].

The response surface in Figure 6 shows a clear interdependence between the applied voltage and the initial substrate concentration on hydrogen production. Voltage is the most influential factor: increasing it from 0.2 V to 1.0 V raises gas production drastically, reaching values close to 400 mL/d. This occurs because voltage acts as the thermodynamic driving force necessary for electrons to overcome the system overpotentials and flow from the anode to the cathode. Increasing the substrate also favors hydrogen production, but its effect tends to stabilize as the concentration increases. This behavior is due to Monod-type saturation kinetics, where the bacteria reach their maximum metabolic processing capacity and the substrate

ceases to be the limiting factor. In the low-voltage zone, H_2 production remains minimal regardless of how much substrate is added, which demonstrates that, without sufficient electrical energy, the biomass cannot channel electrons to the anode effectively. Maximum hydrogen production is reached at 1.0 V and between 6,000 and 8,000 mg/L, because substrate saturation and the minimum internal resistance of the system allow the maximum current flow in the system to be reached. The hydrogen production obtained with the model presents a maximum of 0.4 $m^3/m^3.d$, falling within the same order of magnitude (0.25-0.89 $m^3/m^3.d$) as the results reported in the literature for this type of dual-chamber cell [41], [42], [43], which also validates the selection of the parameters used.

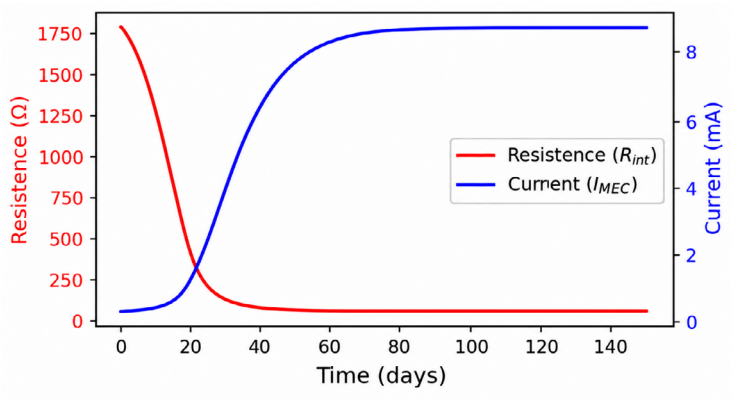

Fig. 5. *Behavior of the internal resistance of an MEC and current production during hydrogen production.*

The response surface for Coulombic efficiency (CE) (Figure 7) reveals a more complex interaction between the applied voltage and the substrate concentration, differing notably from the behavior of hydrogen production. CE reaches its maximum value, above 60%, in a specific region of voltages close to 1.0 V, combined with substrate concentrations around 4,500 mg/L. This behavior indicates that, unlike gas production, conversion efficiency requires a balance where the organic load is high enough to maintain exoelectrogenic activity, but not so excessive as to divert electrons toward competing metabolic pathways such as biomass accumulation.

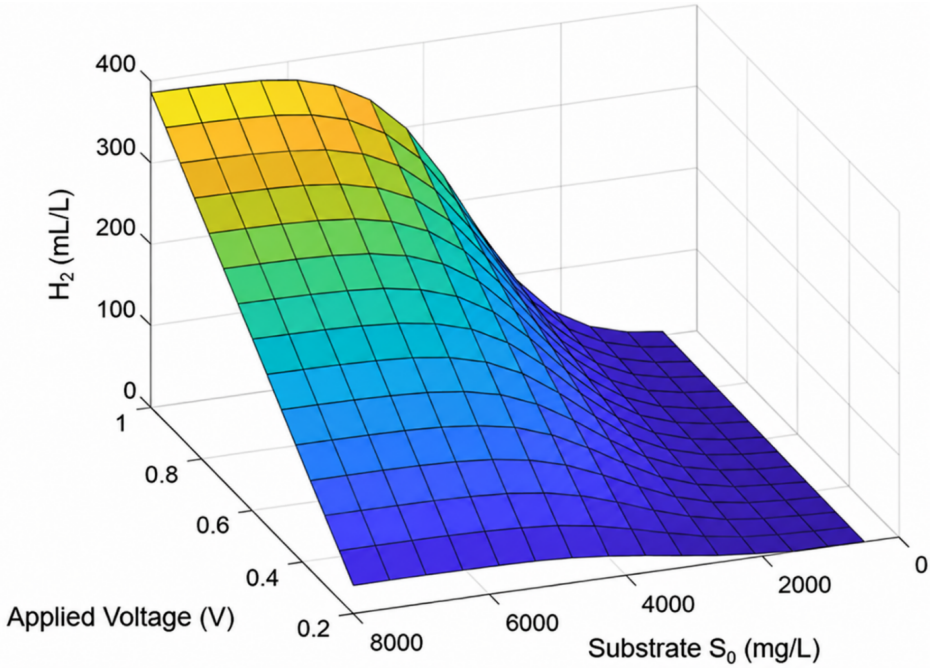

Fig. 6. *Effect of voltage and substrate on hydrogen production in an MEC.*

Efficiency tends to decrease both below and above a substrate concentration of 4,500 mg/L, which suggests that at very low concentrations cell maintenance consumes proportionally more energy, whereas at very high concentrations the electron transfer capacity of the anode becomes saturated. High voltages close to 1.0 V with low or moderate organic loads have been observed to counteract methanogenic activity, favoring the growth kinetics of exoelectrogens, with Coulombic efficiencies

between 21% and 93% reached [44], [45]. When the hydrogen yield on substrate ($Y_{\frac{H_2}{S}}$) is analyzed against changes in voltage and substrate, the response surface shows the same behavior observed for the CE, with a maximum of 150 mL/g at the same optimal conditions. This value lies within the orders of magnitude of the results reported in other studies, which range between 135-340 mL/g [46] and are also similar to those obtained by dark fermentation technologies [47].

The Pareto diagram in Figure 8 indicates that the growth rate of exoelectrogenic bacteria (μ_e), the initial substrate concentration (S_0) and the exponential decay constant of the internal resistance due to the presence of exoelectrogenic population (k_r) are the three parameters with the greatest impact on hydrogen production. The microbiology and metabolism of exoelectrogenic bacteria govern the overall behavior of the cell, as demonstrated by the high sensitivity of the parameters μ_e (growth rate) and q_e (consumption rate), which drive the activity of the biofilm at the anode. The initial substrate concentration S_0, together with the dilution rate D, are additional critical factors representing the flow of electrons available to the system; a limitation in this supply directly restricts the kinetics of hydrogen production by reducing the availability of electron donors.

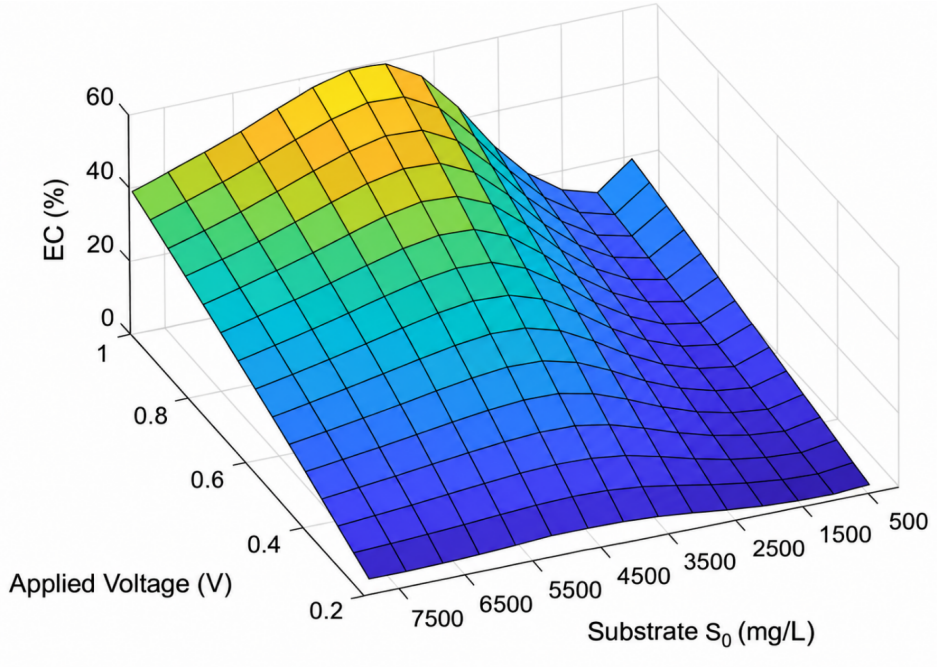

Fig. 7. *Effect of voltage and substrate on the Coulombic efficiency CE of an MEC.*

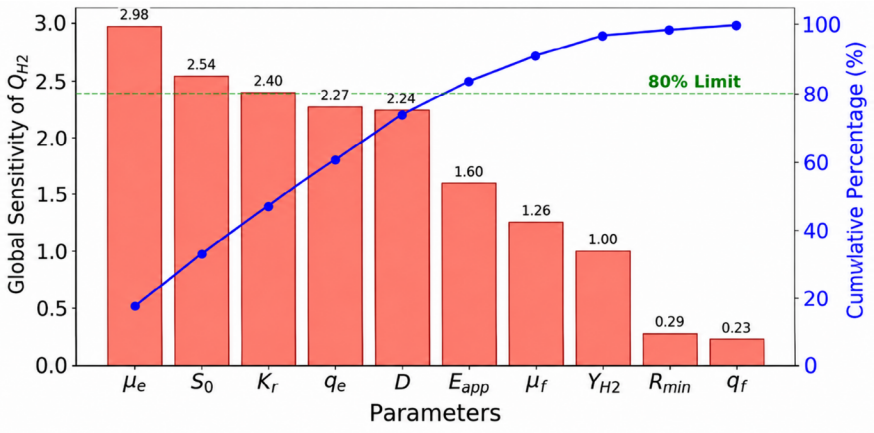

Fig. 8. *Pareto diagram of the model parameters with the greatest effect on hydrogen production*

The Pareto diagram from the global sensitivity analysis for Coulombic efficiency (CE) (Figure 9) again shows that the microbiology and biochemistry of the exoelectrogenic bacteria control the behavior of the cell, since the parameters μ_e and q_e dictate the fraction of substrate that is actually converted into current, while the parameter k_r is a measure of the reduction in internal resistance that facilitates electron transfer to the electrode. The applied voltage E_{app} represents the supplementary energy needed to overcome the thermodynamic barrier of hydrogen production. This parameter is the main modulator of the reaction kinetics, since a higher voltage accelerates the metabolism of the exoelectrogenic biofilm and, therefore, the

intensity of the electric current. At a low voltage, the driving force is weak and the internal resistance dominates; this causes the electrons generated by the bacteria to be diverted toward competitive pathways such as methanogenesis or the synthesis of new biomass, reducing the CE.

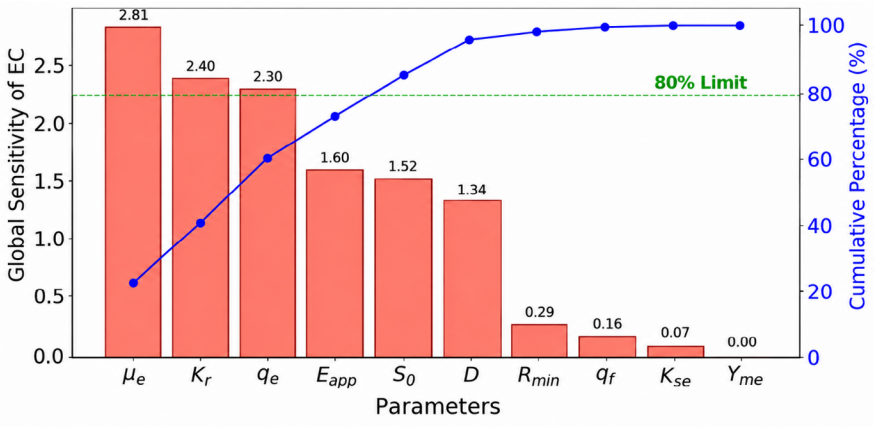

Fig. 9. *Pareto diagram of the model parameters with the greatest effect on hydrogen production and Coulombic efficiency*

CONCLUSIONS

Mathematical modeling is an essential tool for system analysis, allowing prediction of their dynamic behavior and determination of critical parameters; it is fundamental for the design, optimization, and industrial scaling of different technologies.

During the analysis of hydrogen production in an EMF, the main factors observed were the transition of the inoculum to a mature electrogenic biofilm rich in generators that drastically reduces internal resistance, facilitating electronic transfer. Theapplied voltage is one of the most influential factors, achieving productions of up to 400 mL/d of hydrogen at 1.0 V (of 0.4 m^3/m^3 d), reaching Coulombic efficiencies of up to 60%. Sensitivity analyses showed that parameters associated with the biochemistry of the generator cells, such as their growth rate and acetate consumption, applied voltage, and substrate supply, control the overall performance of the cell. Consequently, scaling and optimization should prioritize evaluating these parameters to maximize energy conversion and the economic viability of the process.

REFERENCES

[1] C. Carraro, S. Searle, and C. Baldino, 'Waste and residue availability for advanced biofuel production in the European Union and the United Kingdom', International Council on Clean Transportation, Working paper 2021-39, 2021.

[2] K. Vohra, A. Vodonos, J. Schwartz, E. A. Marais, M. P. Sulprizio, and L. J. Mickley, 'Global mortality from outdoor fine particle pollution generated by fossil fuel combustion: Results from GEOS-Chem', Environmental Research, vol. 195, p. 110754, Apr. 2021, doi: 10.1016/j.envres.2021.110754.

[3] T. da Silva Veras, T. S. Mozer, D. da Costa Rubim Messeder dos Santos, and A. da Silva César, 'Hydrogen: Trends, production and characterization of the main process worldwide', International Journal of Hydrogen Energy, vol. 42, no. 4, pp. 2018–2033, Jan. 2017, doi: 10.1016/j.ijhydene.2016.08.219.

[4] S. G. Nnabuife et al., 'The prospects of hydrogen in achieving net zero emissions by 2050: A critical review', Sustainable Chemistry for Climate Action, vol. 2, p. 100024, Jan. 2023, doi: 10.1016/j.scca.2023.100024.

[5] M. T. Ahad, M. M. H. Bhuiyan, A. N. Sakib, A. B. Corral, and Z. Siddique, 'An Overview of Challenges for the Future of Hydrogen', Materials, vol. 16, no. 20, Oct. 2023, doi: 10.3390/ma16206680.

[6] B. E. Logan et al., 'Microbial Electrolysis Cells for High Yield Hydrogen Gas Production from Organic Matter', ACS Publications. Accessed: Oct. 27, 2022. [Online]. Available: https://pubs.acs.org/doi/pdf/10.1021/es801553z

[7] H. Liu, S. Grot, and B. E. Logan, 'Electrochemically assisted microbial production of hydrogen from acetate', Environ Sci Technol, vol. 39, no. 11, pp. 4317–4320, Jun. 2005, doi: 10.1021/es050244p.

[8] P. Dange et al., 'Recent Developments in Microbial Electrolysis Cell-Based Biohydrogen Production Utilizing Wastewater as a Feedstock', Sustainability, vol. 13, no. 16, Art. no. 16, Jan. 2021, doi: 10.3390/su13168796.

[9] Z. Dai, E. S. Heidrich, J. Dolfing, and A. P. Jarvis, 'Determination of the Relationship between the Energy Content of Municipal Wastewater and Its Chemical Oxygen Demand', Environ. Sci. Technol. Lett., vol. 6, no. 7, pp. 396–400, Jul. 2019, doi: 10.1021/acs.estlett.9b00253.

[10] E. S. Heidrich, T. P. Curtis, and J. Dolfing, 'Determination of the Internal Chemical Energy of Wastewater', Environ. Sci. Technol., vol. 45, no. 2, pp. 827–832, Jan. 2011, doi: 10.1021/es103058w.

[11] B. E. Logan and K. Rabaey, 'Conversion of wastes into bioelectricity and chemicals by using microbial electrochemical technologies',

Science, vol. 337, no. 6095, pp. 686–690, Aug. 2012, doi: 10.1126/science.1217412.

[12] E. Yang et al., 'A review on self-sustainable microbial electrolysis cells for electro-biohydrogen production via coupling with carbon-neutral renewable energy technologies', Bioresource Technology, vol. 320, p. 124363, Jan. 2021, doi: 10.1016/j.biortech.2020.124363.

[13] G. Kumar et al., 'Microbial electrochemical systems for sustainable biohydrogen production: Surveying the experiences from a start-up viewpoint', Renewable and Sustainable Energy Reviews, vol. 70, pp. 589–597, Apr. 2017, doi: 10.1016/j.rser.2016.11.107.

[14] M. Muddasar et al., 'Performance efficiency comparison of microbial electrolysis cells for sustainable production of biohydrogen—A comprehensive review', International Journal of Energy Research, vol. 46, no. 5, pp. 5625–5645, 2022, doi: 10.1002/er.7606.

[15] S. Gadkari, S. Gu, and J. Sadhukhan, 'Towards automated design of bioelectrochemical systems: A comprehensive review of mathematical models', Chemical Engineering Journal, vol. 343, no. February, pp. 303–316, 2018, doi: 10.1016/j.cej.2018.03.005.

[16] R. P. Pinto, B. Srinivasan, A. Escapa, and B. Tartakovsky, 'Multi-Population Model of a Microbial Electrolysis Cell', Environ. Sci. Technol., vol. 45, no. 11, pp. 5039–5046, Jun. 2011, doi: 10.1021/es104268g.

[17] S. Gadkari, M. Shemfe, and J. Sadhukhan, 'Microbial fuel cells: A fast converging dynamic model for assessing system performance based on bioanode kinetics', International Journal of Hydrogen Energy, vol. 44, no. 29, pp. 15377–15386, Jun. 2019, doi: 10.1016/j.ijhydene.2019.04.065.

[18] X.-C. Zhang and A. Halme, 'Modelling of a microbial fuel cell process', Biotechnol Lett, vol. 17, no. 8, pp. 809–814, Aug. 1995, doi: 10.1007/BF00129009.

[19] R. P. Pinto, B. Srinivasan, M.-F. Manuel, and B. Tartakovsky, 'A two-population bio-electrochemical model of a microbial fuel cell', Bioresource Technology, vol. 101, no. 14, pp. 5256–5265, Jul. 2010, doi: 10.1016/j.biortech.2010.01.122.

[20] M. Kazemi, D. Biria, and H. Rismani-Yazdi, 'Modelling bio-electrosynthesis in a reverse microbial fuel cell to produce acetate from CO2 and H2O', Phys. Chem. Chem. Phys., vol. 17, no. 19, pp. 12561–12574, 2015, doi: 10.1039/c5cp00904a.

[21] Q. Ping, C. Zhang, X. Chen, B. Zhang, Z. Huang, and Z. He, 'Mathematical Model of Dynamic Behavior of Microbial Desalination Cells for Simultaneous Wastewater Treatment and Water Desalination', Environ. Sci. Technol., vol. 48, no. 21, pp. 13010–13019, Nov. 2014, doi: 10.1021/es504089x.

[22] S. Yao, Y.-L. He, B.-Y. Song, and X.-Y. Li, 'A two-dimensional, two-phase mass transport model for microbial fuel cells', Electrochimica Acta, vol. 212, pp. 201–211, Sep. 2016, doi: 10.1016/j.electacta.2016.06.167.

[23] C. Picioreanu, M. C. M. van Loosdrecht, T. P. Curtis, and K. Scott, 'Model based evaluation of the effect of pH and electrode geometry on microbial fuel cell performance', Bioelectrochemistry, vol. 78, no. 1, pp. 8–24, Apr. 2010, doi: 10.1016/j.bioelechem.2009.04.009.

[24] Y. Azwar, A. K. Abdul-Wahab, and M. A. Hussain, 'Optimal Production of Biohydrogen Gas via Microbial Electrolysis Cells (MEC) in a Controlled Batch Reactor System'.

[25] A. M. Yahya, M. A. Hussain, and A. K. Abdul Wahab, 'Modeling, optimization, and control of microbial electrolysis cells in a fed-batch reactor for production of renewable biohydrogen gas', International Journal of Energy Research, vol. 39, no. 4, pp. 557–572, 2015, doi: 10.1002/er.3273.

[26] B. Sirinutsomboon, 'Modeling of a membraneless single-chamber microbial fuel cell with molasses as an energy source', Int. J. Energy Environ. Eng., vol. 5, no. 2–3, pp. 1–9, 2014, doi: 10.1007/s40095-014-0093-5.

[27] Y. Zeng, Y. F. Choo, B.-H. Kim, and P. Wu, 'Modelling and simulation of two-chamber microbial fuel cell', Journal of Power Sources, vol. 195, no. 1, pp. 79–89, Jan. 2010, doi: 10.1016/j.jpowsour.2009.06.101.

[28] V. B. Oliveira, M. Simões, L. F. Melo, and A. M. F. R. Pinto, 'A 1D mathematical model for a microbial fuel cell', Energy, vol. 61, pp. 463–471, Nov. 2013, doi: 10.1016/j.energy.2013.08.055.

[29] M. N. Ikhmal Salehmin et al., 'Modeling biohydrogen production from microbial electrolysis cells in the machine learning era: a review', Sustainable Energy Technologies and Assessments, vol. 85, p. 104819, Jan. 2026, doi: 10.1016/j.seta.2026.104819.

[30] M. A. Mohd Asrul, M. F. Atan, H. Abdul Halim Yun, and J. C. H. Lai, 'Mathematical model of biohydrogen production in microbial electrolysis cell: A review', International Journal of Hydrogen Energy, vol. 46, no. 75, pp. 37174–37191, Oct. 2021, doi: 10.1016/j.ijhydene.2021.09.021.

[31] A. Garg, V. Vijayaraghavan, S. S. Mahapatra, K. Tai, and C. H. Wong, 'Performance evaluation of microbial fuel cell by artificial intelligence methods', Expert Systems with Applications, vol. 41, no. 4, Part 1, pp. 1389–1399, Mar. 2014, doi: 10.1016/j.eswa.2013.08.038.

[32] E. M. Conners, K. Rengasamy, and A. Bose, 'Electroactive biofilms: how microbial electron transfer enables bioelectrochemical applications', J. Ind. Microbiol. Biotechnol., vol. 49, no. 4, p. kuac012, Jul. 2022, doi: 10.1093/jimb/kuac012.

[33] C. Montoya-Vallejo, J. O. Gil Posada, and J. C. Quintero-Díaz, 'Enhancement of Electricity Production in Microbial Fuel Cells Using a Biosurfactant-Producing Co-Culture', Molecules, vol. 28, no. 23, Art. no. 23, Jan. 2023, doi: 10.3390/molecules28237833.

[34] E. Marsili, D. B. Baron, I. D. Shikhare, D. Coursolle, J. A. Gralnick, and D. R. Bond, 'Shewanella secretes flavins that mediate extracellular electron transfer', Proceedings of the National Academy of Sciences, vol. 105, no. 10, pp. 3968–3973, Mar. 2008, doi: 10.1073/pnas.0710525105.

[35] A. Kato Marcus, C. I. Torres, and B. E. Rittmann, 'Conduction-based modeling of the biofilm anode of a microbial fuel cell', Biotechnology and Bioengineering, vol. 98, no. 6, pp. 1171–1182, 2007, doi: 10.1002/bit.21533.

[36] A. Saltelli, M. Ratto, S. Tarantola, and F. Campolongo, 'Sensitivity Analysis for Chemical Models', Chem. Rev., vol. 105, no. 7, pp. 2811–2828, Jul. 2005, doi: 10.1021/cr040659d.

[37] A. Varma, M. Morbidelli, and H. Wu, Parametric sensitivity in chemical systems, vol. 1. Cambridge University Press Cambridge, 1999.

Accessed: Mar. 22, 2026. [Online]. Available: https://www.academia.edu/download/118001995/248350749.pdf

[38] W. Cai et al., 'Biocathodic Methanogenic Community in an Integrated Anaerobic Digestion and Microbial Electrolysis System for Enhancement of Methane Production from Waste Sludge', ACS Sustainable Chem. Eng., vol. 4, no. 9, pp. 4913–4921, Sep. 2016, doi: 10.1021/acssuschemeng.6b01221.

[39] J. C. Quintero-Díaz and J. O. Gil-Posada, 'Batch and semi-continuous treatment of cassava wastewater using microbial fuel cells and metataxonomic analysis', Bioprocess Biosyst Eng, vol. 47, no. 7, pp. 1057–1070, Jul. 2024, doi: 10.1007/s00449-024-03025-0.

[40] S. J. Satinover, M. Rodriguez, M. F. Campa, T. C. Hazen, and A. P. Borole, 'Performance and community structure dynamics of microbial electrolysis cells operated on multiple complex feedstocks', Biotechnol Biofuels, vol. 13, no. 1, p. 169, Oct. 2020, doi: 10.1186/s13068-020-01803-y.

[41] P. Batlle-Vilanova et al., 'Assessment of biotic and abiotic graphite cathodes for hydrogen production in microbial electrolysis cells', International Journal of Hydrogen Energy, vol. 39, no. 3, pp. 1297–1305, Jan. 2014, doi: 10.1016/j.ijhydene.2013.11.017.

[42] L. Lu, D. Xing, N. Ren, and B. E. Logan, 'Syntrophic interactions drive the hydrogen production from glucose at low temperature in microbial electrolysis cells', Bioresource Technology, vol. 124, pp. 68–76, Nov. 2012, doi: 10.1016/j.biortech.2012.08.040.

[43] L. Cristiani et al., 'Enhancing energy efficiency and H2 production in lab-scale dual chamber microbial electrolysis cells: A focus on catholyte composition and voltage losses', Journal of Environmental Chemical Engineering, vol. 12, no. 1, p. 111782, Feb. 2024, doi: 10.1016/j.jece.2023.111782.

[44] T. H. J. A. Sleutels, S. D. Molenaar, A. T. Heijne, and C. J. N. Buisman, 'Low Substrate Loading Limits Methanogenesis and Leads to High Coulombic Efficiency in Bioelectrochemical Systems', Microorganisms, vol. 4, no. 1, Jan. 2016, doi: 10.3390/microorganisms4010007.

[45] I. Ivanov, L. Ren, M. Siegert, and B. E. Logan, 'A quantitative method to evaluate microbial electrolysis cell effectiveness for energy recovery and wastewater treatment', International Journal of Hydrogen Energy, vol. 38, no. 30, pp. 13135–13142, Oct. 2013, doi: 10.1016/j.ijhydene.2013.07.123.

[46] L. Zhang, Y. Bai, J. Sang, J. Dong, X. Wu, and Q. Ban, 'Enhanced Biohydrogen Production through Dark Fermentation by Humic Acid: Insights into Microbial Composition and Functional Genes', J Microbiol Biotechnol, vol. 35, p. e2412071, Jun. 2025, doi: 10.4014/jmb.2412.12071.

[47] R. Abdallah et al., 'Dark fermentative hydrogen production by anaerobic sludge growing on glucose and ammonium resulting from nitrate electroreduction', International Journal of Hydrogen Energy, vol. 41, no. 12, pp. 5445–5455, Apr. 2016, doi: 10.1016/j.ijhydene.2016.02.030.

FUNDING

No financing

CONFLICT OF INTEREST

None

AUTHORSHIP CONTRIBUTIONS

Drafting – original draft: Juan Carlos Quintero Díaz, Diego Fernando Mendoza Muñoz.

Writing–review and editing: Juan Carlos Quintero Díaz, Diego Fernando Mendoza Muñoz.